

International Conference on “Recent trends in Mechanical Engineering” (ICRTME-2007), October 4-6, 2007, Ujjain Engineering College Ujjain (M.P.), India

CFD SIMULATION OF ORIFICE PULSE TUBE REFRIGERATOR

Banjare Y. P. *, Sahoo R. K., Sarangi S. K.

Department of Mechanical Engineering, NIT Rourkela-769008, Orissa

***Corresponding Author:** e-mail: yp_banjare@yahoo.co.in

Abstract

A commercial Computational fluid dynamics (CFD) software package Fluent 6.1 is used to model the oscillating flow inside a pulse tube cryocooler. In this paper analysis of orifice type pulse tube refrigerator (OPTR) systems operating under a variety of thermal boundary conditions are modeled at different frequencies. The compressor used is having dual opposed piston arrangement. The simulations are done at different frequencies with helium as working fluid. The simulated OPTR consists of a compressor (dual opposed piston), a transfer line, an after cooler, a regenerator, a pulse tube, a pair of heat exchangers for cold and hot end, an orifice valve and a reservoir. The simulation represents fully coupled systems operating in steady-periodic mode. The externally imposed boundary conditions are a cyclically moving piston wall at one end of the tube and constant temperature or heat flux boundaries at the external walls of the hot end and cold end heat exchangers. The experimental method to evaluate the optimum parameters of OPTR is difficult. On the other hand, developing a computer code for CFD analysis is equally complex. The objectives of the present investigation are to ascertain the suitability of CFD based commercial package, Fluent and also to examine the performance for the effect of compressor frequency on the orifice type pulse tube refrigerator (OPTR). The results confirm that CFD based Fluent simulations are capable of elucidating complex periodic processes in OPTRs. As a result, the performance analysis also shows that an optimum frequency always exists corresponding to the minimum cold end temperature for same operating boundary conditions. Results show that at high frequency the secondary-flow recirculation occur at the vicinity of component-to-component junctions to reduce the heat pumping effect from low temperature heat exchanger (HX) to high temperature HX. On the contrary, at low frequency, the low pumping rate affects to achieve the minimum temperature. Hence the system performance is best achieved at an optimum frequency.

Keywords: Orifice pulse tube refrigerator; dual opposed piston compressor, Regenerator; CFD

Nomenclature

\overline{C}	Inertial drag coefficient tensors (m^{-1})
h	Enthalpy (J/kg)
j	Superficial velocity (m/s)
k	Thermal conductivity (W/m K)
p	Pressure (N/m^2)
T	Temperature (k)
t	Time (s)
v	Intrinsic velocity (m/s)
ω	Angular frequency (rad/s)
X	Piston displacement (m)
X_a	Piston displacement amplitude (m)
$\langle \dot{H} \rangle$	Average enthalpy flow rate over a cycle (W)
C_p	Specific gas constant, (J/kg-K)
Period	Period of the cycle(s)

Greek letters

$\overline{\beta}$	Permeability tensors (m^2)
ϕ	Porosity
θ	Angle
α_1, α_2	Phase angle
μ	absolute viscosity (kg/m s)
ρ	density (kg/m^3)
$\overline{\tau}$	Stress tensors (N/m^2)
F	Frequency

Subscripts

f	fluid
---	-------

r	radial coordinate
s	solid
x	axial coordinate

Introduction

Basic pulse tube refrigerator (BPTR) was originally proposed by Gifford and Longworth [1] in 1964. Mukuline et al. [2] made an important improvement by adding an orifice valve between pulse tube and reservoir to improve the performance of BPTR. This modification leads to orifice pulse tube refrigerator (OPTR). Zhu et al. [3] proposed a double inlet pulse tube refrigerator (DIPTR) by adding a double inlet valve in an orifice pulse tube refrigerator, which improved the refrigeration performance significantly. The major design variations introduced so far include the modified OPTR [4], the multi-pass OPTR [5], and most recently the inertance tube pulse tube refrigerator (ITPTR) [6]. The exact nature of the physical phenomena underlying the operation of PTRs is not well-understood, [7, 8]. Multidimensional flow effect has been analysed by Cha et al. [10] by taking single piston linear compressor at constant frequency. They have not mentioned the effect of frequency on ITPTR performance. In the present work a dual opposed piston compressor is used for analysis and also the effect of compressor frequency is studied. The difficulty in all PTRs is that their working fluid compression and expansion processes are not well-defined, and poorly-understood thermal relaxation and phase-lag phenomena dominate their operation. Crucial among these is the phase angle between pressure and mass flow. This phase angle is influenced by the wave resonance phenomena in BPTRs, and is adjusted by orifices and/or valves in various OPTR designs. In an ITPTR, the orifice valve of the simple OPTR is replaced by an Inertance tube that, with proper design, can cause an optimal phase lag between pressure and mass flow rate in the pulse tube. Because of their simple construction pulse tube refrigeration provides attractive applications, ranging from cooling the infrared sensors for aerospace applications, and semiconductors and superconducting magnets, space vehicles at cryogenic temperature to the cooling of other civilian appliances at higher temperature.

Simulated systems

The numerical experiment based on Fluent 6.1, is focused on the multidimensional flow effect and phase relationship for performance evaluation of OPTR at different frequencies of the dual compressor for helium gas as working fluid. The experimental analysis of OPTR for varying design and operating condition is difficult. It is also equally complex to develop a numerical code for CFD analysis consisting of compressor and other passive components. Hence the primary aim of this

investigation is to ascertain the suitability of available commercial CFD, Fluent 6.1 software for numerical experimentation. The secondary aim of this investigation is to study the effect of frequency on the performance of an OPTR driven by the widely used dual opposed piston compressor.

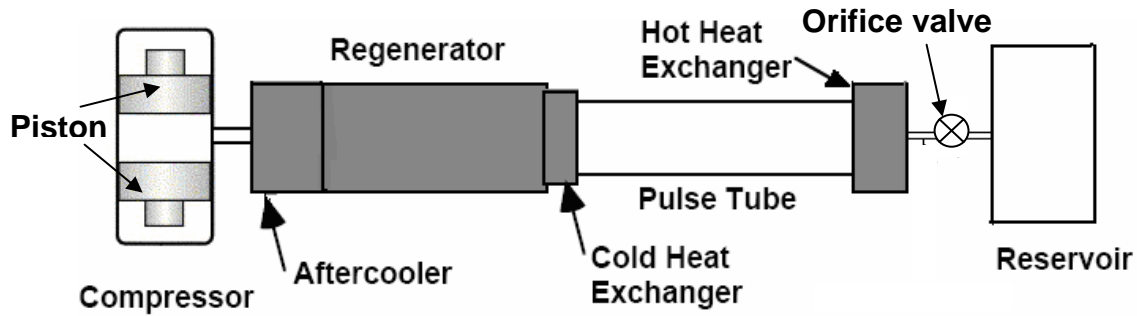


Fig.1: Schematics of orifice pulse tube refrigerator with dual oppose piston compressor.

A schematic of the OPTR system is shown in Fig. 1. The geometry of the system are same as Cha et al. [10] except that the present model uses a dual opposed piston compressor. The radius of compressor is $9.54 \times 10^{-3} \text{m}$ and length is $7.5 \times 10^{-3} \text{m}$, transfer line radius is $1.55 \times 10^{-3} \text{m}$ and length is 0.101m , after cooler radius is $4.00 \times 10^{-3} \text{m}$ and length is 0.02m , regenerator radius is $4.00 \times 10^{-3} \text{m}$ and length is 0.58m , cold end heat exchanger radius is $3.00 \times 10^{-3} \text{m}$ and length is 0.0057m , hot end heat exchanger radius is $4.00 \times 10^{-3} \text{m}$ and length is 0.06m , orifice tube radius is 0.0005m and length is 0.13m and surge volume radius is $1.30 \times 10^{-2} \text{m}$ and length is 0.13m . The two dimensional axisymmetric geometry is taken for simulation. The mirror view of axi-symmetric geometry with complete mesh is shown in Fig.2.

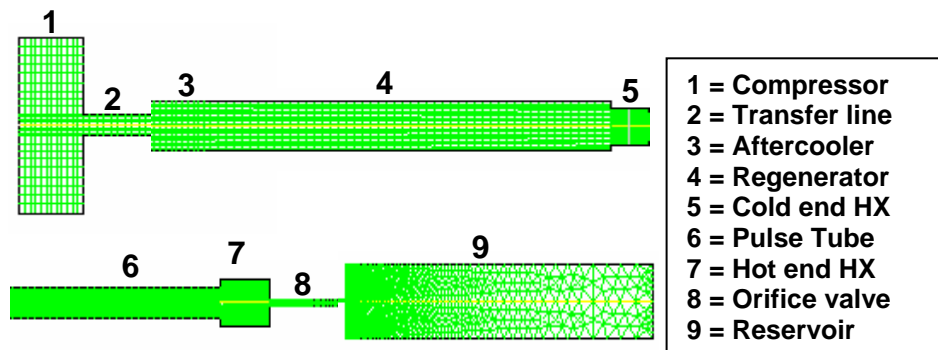


Fig. 2: Two-Dimensional Mesh for orifice pulse tube refrigerator (Mirror view)

Boundary conditions for the simulations:

The pulse tube system model is simulated for three different operational modes to compare their performances. The three cases address operation with an adiabatic cold end heat exchanger (i.e., zero cooling loads), a specified cold end cooling load of 1W (known heating load), and a known cold end temperature of 150K (Isothermal condition). For the above cases the after cooler wall and hot end heat exchanger are maintained at 293K (Isothermal condition).The other parts of the system are insulated.

The piston head motion of the compressor is modeled as simple user defined function (UDF) as

$$\text{Piston displacement} = X = X_a \sin(\omega t) \quad (1)$$

$$\text{Piston head velocity} = V = \frac{dX}{dt} = X_a \omega \cos(\omega t) \quad (2)$$

Where $\omega = 2 * \pi * F$ [rad/s], F = frequency.

$X_a = 4.5 \times 10^{-3}$ [m] and time increment of 7.3529×10^{-4} second was assumed for all cases.

Fluent is equipped with a dynamic meshing function that can create deformable mesh volumes based on the above UDF to model the reciprocating motion of the compressor. Detailed nodalization of all components is performed, whereby regions deemed more sensitive, such as the vicinity of component-to-component junctions, are represented by finer mesh than others.

Governing equations:

Continuum-based conservation equations can be applied everywhere in the system. The mass, momentum and energy equations solved by fluent are as follows

$$\frac{\partial \rho_f}{\partial t} + \frac{1}{r} \frac{\partial}{\partial r} (r \rho_f V_r) + \frac{\partial}{\partial x} (\rho_f V_x) = 0 \quad (3)$$

$$\frac{\partial}{\partial t} (\rho_f \vec{v}) + \nabla (\rho_f \vec{v} \vec{v}) = -\nabla p + \nabla \cdot \left[\underline{\underline{\tau}} \right] \quad (4)$$

$$\frac{\partial}{\partial t} (\rho_f E) + \nabla \cdot [\vec{v} (\rho_f E + p)] = \nabla \cdot \left[k_f \nabla T + \left(\underline{\underline{\tau}} \cdot \vec{v} \right) \right] \quad (5)$$

$$\text{Where } E = h - \frac{p}{\rho} + \frac{v^2}{2} \quad (6)$$

All properties represent the properties of the working fluid helium. The above equations apply to all components, except for aftercooler, cold heat exchanger, hot heat exchanger and to the regenerator. The latter four components are modeled as porous media, assuming that there is local thermodynamic equilibrium between the fluid and solid structure in these components. The mass, momentum, and energy equations in the latter four components are:

$$\frac{\partial(\phi\rho_f)}{\partial t} + \frac{1}{r} \frac{\partial}{\partial r}(\phi r \rho_f V_r) + \frac{\partial}{\partial x}(\phi \rho_f V_x) = 0 \quad (7)$$

$$\frac{\partial}{\partial t}(\phi \rho_f \bar{v}) + \nabla(\phi \rho_f \bar{v} \bar{v}) = -\phi \nabla p + \nabla \cdot [\phi \bar{\tau}] - \left(\mu \bar{\beta}^{-1} \cdot \bar{j} + \frac{1}{2} \bar{C} \rho_f |\bar{j}| \bar{j} \right) \quad (8)$$

$$\frac{\partial}{\partial t}(\phi \rho_f E_f + (1-\phi) \rho_s E_s) + \nabla \cdot [\bar{v}(\rho_f E_f + p)] = \nabla \cdot [\phi k_f + (1-\phi) \nabla T + (\phi \bar{\tau} \cdot \bar{v})] \quad (9)$$

Where $\phi = 0.69$, $\bar{\beta} = 1.06 \times 10^{-10} \text{ [m}^2\text{]}$ and $\bar{C} = 76090 \text{ [m}^{-1}\text{]}$ were assumed. These parameters are based on experiments of Harvey [9] for axial flow through a randomly packed stack of 325 mesh stainless steel screens.

Since pulse tube is under adiabatic condition, the maximum enthalpy flow from cold end to hot end heat exchanger gives the best cooling performance of OPTR. The average enthalpy flow rate over a cycle is,

$$\langle \dot{H} \rangle = \frac{1}{\text{Period}} \int \dot{m} T \cos \theta C_p dt \quad (10)$$

In this expression \dot{m} and T are phaser quantities where \dot{m} is the cross-sectional average mass flow rate and T is the mass averaged temperature at the same spatial location. For maximum enthalpy flow rate both of these phasors should be in same phase ($\cos \theta = 1$) with their maximum amplitudes.

Result and discussion

The pulse tube system model has been simulated with different boundary conditions as specified earlier for frequencies 10,20,30,40 and 50Hz. In order to study the refrigeration performance,

results of steady periodic CFD simulation with adiabatic boundary condition are presented. It has been observed that results of other boundary conditions give similar performance.

The cyclic average temperature variation at cold end with time for different frequencies is shown in Fig.3. However, it should be emphasized that in actual system, the cooling time will be higher than that has been predicted in this result since the thermal mass has not been taken into consideration.

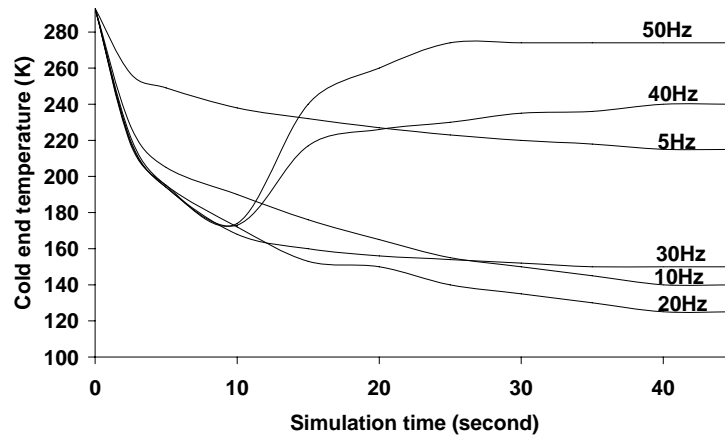


Fig.3: Cool down behavior at different frequency frequency

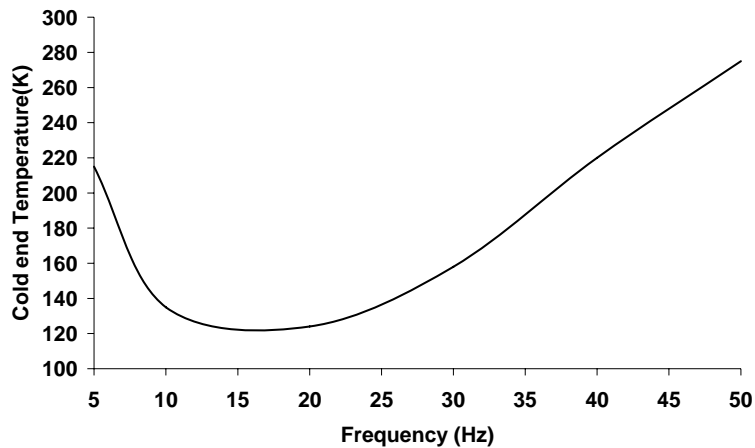


Fig.4: Cold end Temperature verses frequency

It has been observed from Fig.3 that there is an optimum frequency for the minimum cold end temperature which is shown in Fig.4. This is because when the frequency decreases, the thickness of the thermal viscous layer will increase, and eventually the gross refrigeration power will decrease more than the regenerator inefficiency loss, this will lead to an increase in cold end temperature. Similarly when frequency increases the thermal viscous layer will decrease, and the increase of refrigeration power will eventually be surpassed by that of the regenerator inefficiency loss, which will also lead to

an increase of the cold end temperature. Therefore, at a certain frequency, the cold end temperature is the lowest. From thermodynamic point of view the average enthalpy flow over a cycle should be maximum at the optimum frequency as shown in equation (10). This phenomenon is illustrated in Fig.5 by considering the phase lag and amplitude at 20Hz and 30Hz. The phase angles are α_1 and α_2 at 20Hz and 30 Hz respectively. It can be concluded that amplitude of the phasor quantities always decreases with increasing frequency but their phase angle undergoes a minimum.

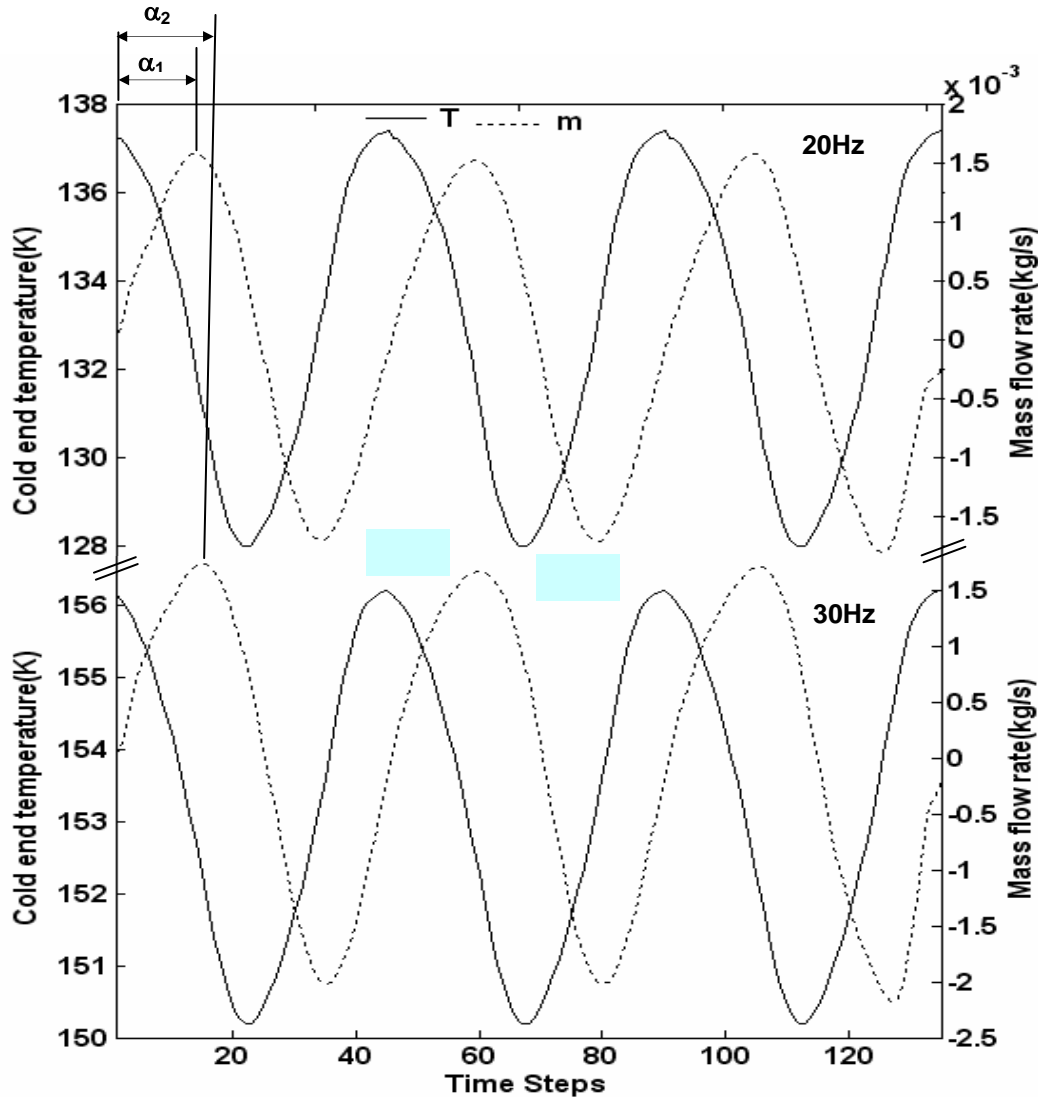


Fig.5: Combined Phase relations for 20 Hz and 30 Hz frequency

The temperature and density contour along the length of the simulated system is shown in Fig.6 and Fig.7 respectively. Similarly the temperature and density distribution along the length of the simulated system are shown in Fig.8 and Fig.9 respectively. In this simulation, the entire system was initially at 293 K. Once steady periodic state is achieved, the cold end is stabilized at 129K at 20 Hz frequency. In the depicted simulation, to verify that the system has reached steady periodic condition, Fluent examines the cold end to see if the temperature of the cold end is identically repeated from one

cycle to the next. However, the temperature and density profile depicts a local instantaneous snapshot of the system.

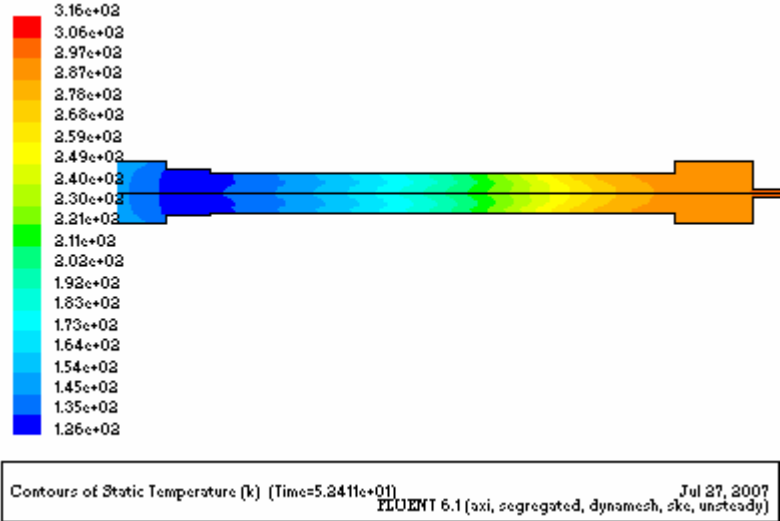


Fig.6: Temperature contour along axial direction for adiabatic cold end condition

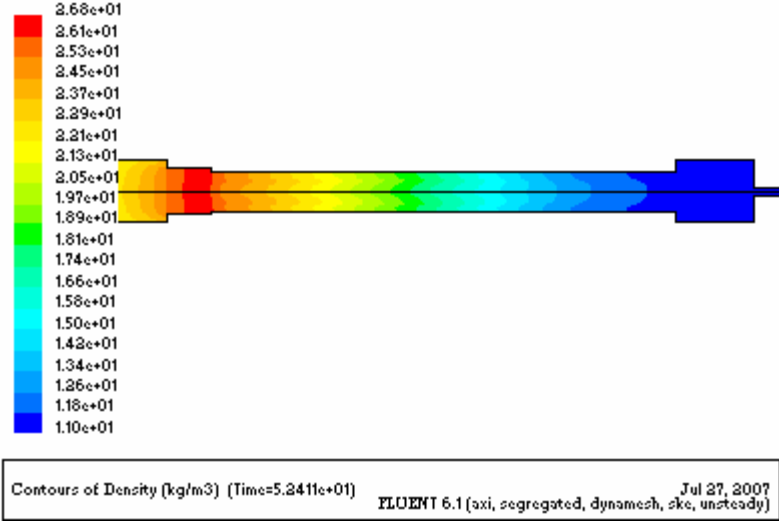


Fig.7: Density contour along axial direction for adiabatic cold end condition

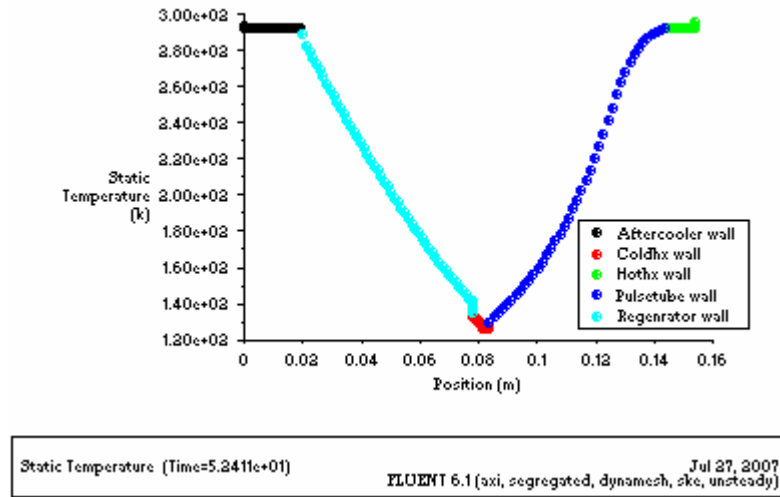


Fig.8: Temperature distributions along axial direction for adiabatic cold end condition

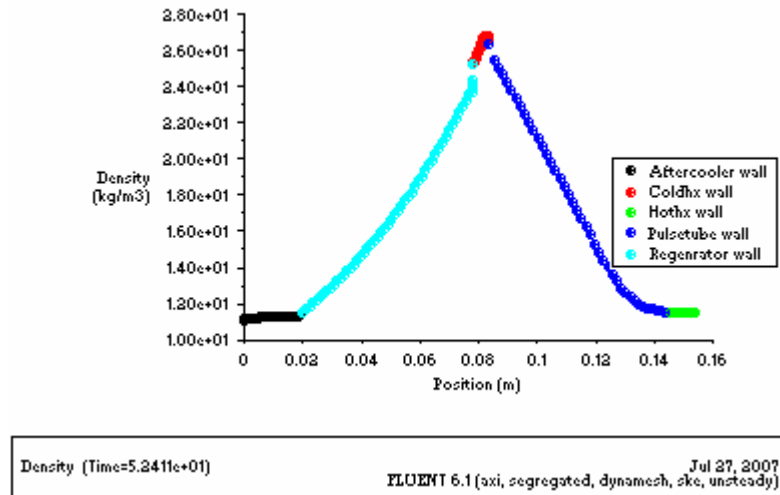


Fig.9: Density distributions along axial direction for adiabatic cold end

Fig.10 shows the velocity vector at pulse tube section at 20 Hz. It is clear from the velocity vector that there are no vortices and recirculation pattern to deteriorate the performance at medium frequency of 20Hz. But Fig.11 shows that at 50 Hz frequency vortices and recirculation pattern are observed at pulse tube section which deteriorate the performance of the system and cold end temperature stabilized at a higher temperature of 270K.

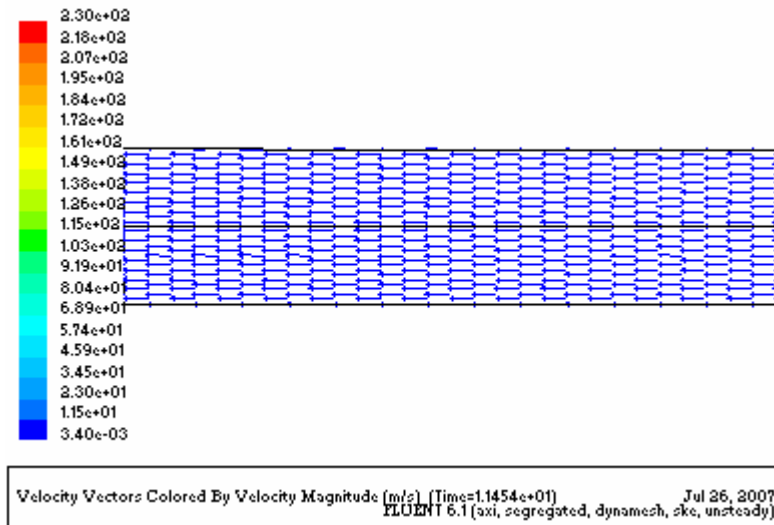


Fig.10: Velocity vector at pulse tube section at 20 Hz frequency

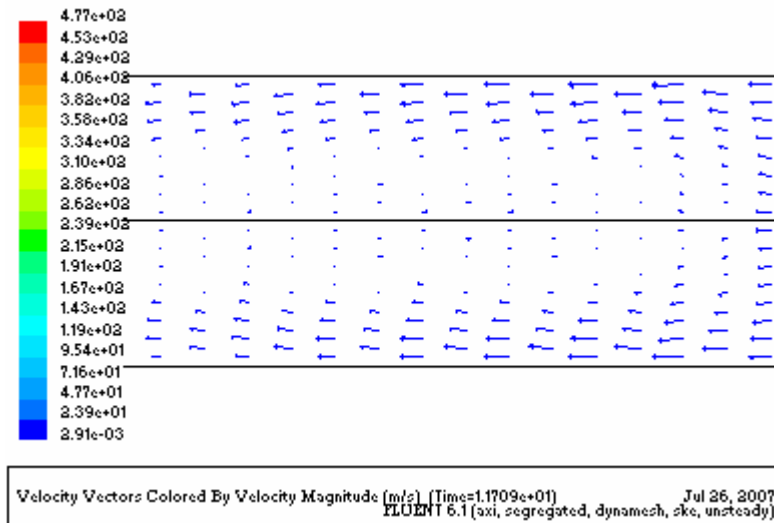


Fig.11: Velocity vector at pulse tube section at 50 Hz frequency

Conclusions

Orifice pulse tube refrigerator systems, operating in steady periodic state under a variety of boundary conditions, are numerically simulated, for different frequencies of compressor using the CFD package, Fluent6.1 [12]. The objectives were to demonstrate the feasibility of CFD simulation of PTRs, and also to examine the performance of OPTR at different frequencies. The CFD simulations successfully predict all the expected trends. They also show that at high frequency the amplitude of mass flow rate and temperature is less with significant fluid recirculation. It has been also observed

that an optimum frequency always exists, corresponding to the minimum cold end temperature for each operating condition.

References

- [1] Gifford W, Longworth R. Pulse-tube refrigeration. *Trans ASME, J Eng Ind (series B)* 1964; 86:264–8.
- [2] Mikulin E, Tarasov A, Shrebyonock M. Low-temperature expansion pulse tubes. *Adv Cryogen Eng* 29:629–37.
- [3] Zhu S, Wu P, Chen Z. A single stage double inlet pulse tube refrigerator capable of reaching 42 K. *ICEC 13 Proc Cryogenics* 1990; 30:256–61.
- [4] Wang C, Wu P, Chen Z. Modified orifice pulse tube refrigerator without a reservoir. *Cryogenics* 1994; 34:31–6.
- [5] Cai J, Wang J, Zhu W, Zhou Y. Experimental analysis of double-inlet principle in pulse tube refrigerator. *Cryogenics* 1993; 33:522–5.
- [6] Zhu S, Zhou S, Yoshimura N, Matsubara Y. Phase shift effect of the long neck tube for the pulse tube refrigerator. In: *Proceedings of the 9th international cryocoolers conference*, June 1996. p. 269-76.
- [7] Richardson R, Evans B. A review of pulse tube refrigeration. *Int J Refrig* 1997; 20:367–73.
- [8] Popescu G, Radenco V, Gargalian E, Bala P. A critical review of pulse tube cryogenerator research. *Int J Refrig* 2001; 24:230–7.
- [9] Harvey J. Parametric study of cryocooler regenerator performance, MS Thesis, Georgia Institute of Technology, Atlanta, GA, 1999.
- [10] Cha J. S., Ghiaasiaan S.M., Multi-dimensional flow effects in pulse tube refrigerators. *Cryogenics* 46 (2006), pp658-665.
- [11] Flake B., Razani A., Modeling Pulse Tube Cryocoolers with CFD. In: *Proceedings of the International Cryogenics Engineering Conference*, September 2003, pp.1493-99
- [12] Fluent INC. *Fluent 6 User Manual*, Fluent INC: 2003 pp. 8-1.
- [13] Lu G. Q., Numerical and Experimental Study of a Gifford- McMahon –Type Pulse Tube Refrigerator. *Journal of Thermophysics and Heat Transfer* Vol. 17 No. 4, October –December 2003, pp. 457-463.